Comparative Study of Conformational and Kinetic Data Concerning Excimer Formation in Models for Poly(1-vinylpyrene)

Paul Collart, Suzanne Toppet, Q. F. Zhou, Noël Boens, and F. C. De Schryver*

Department of Chemistry, University of Leuven, Celestijnenlaan 200 F, 3030 Leuven (Heverlee), Belgium. *Received July 30, 1984*

ABSTRACT: A conformational analysis of *meso*- and *rac*-2,4-di(1-pyrenyl)pentane (D1PP) is performed by using ^{1}H NMR spectroscopy. Conformational effects were studied as a function of temperature and solvent. Conformational information concerning *meso*- and *rac*-bis[1-(1-pyrenyl)ethyl] ether (B1PEE) is given by using ^{1}H NMR and ^{13}C NMR spectroscopy and a comparative study with D1PP is performed. Spectral and time-dependent fluorescence properties of *meso*-D1PP and *meso*-B1PEE were compared.

Introduction

Photophysics of polyvinyl polymers with pendant aromatic groups is a much investigated research field. To elucidate the complex excited-state kinetic behavior of these polymers one can do experiments on the polymer as such[1-3] or one can use model compounds.[4-12] Diastereomeric model compounds of the type shown in I are in this

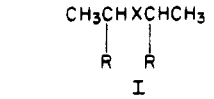

I

Ia, R = phenyl, X = CH_2
Ib, R = 1-naphthyl, X = O
Ic, R = 2-naphthyl, X = O, CH_2
Id, R = *N*-carbazolyl, X = CH_2

approach interesting to understand the emissive behavior of the polymers with respect to excimer formation. The substantial difference of the excited-state properties of *meso*- and *rac*-2,4-diphenylpentane (Ia) has been pointed out by Monnerie and Bovey.[13] The capacity to form excimer is quite different for these diastereoisomers. The reason for this difference can be found in the conformational distribution within each configuration.[12] Similar observations have been made for the other chromophores shown in I.[6-10] The excimer-forming process is governed by two factors: (a) the possibility to form an excimer through conformational changes within the lifetime of the chromophore and (b) the thermodynamic stability of the excimer.[4] It is therefore of major importance to obtain information on the conformational aspects of these molecules and to link these with their photophysical behavior. The former information can be gained by NMR studies,[14-16] by infrared spectrocopy,[17] or by a more theoretical approach.[18-20] In this report we want to compare ground- and excited-state behavior of 2,4-di(1-pyrenyl)pentane (D1PP) with that of bis[1-(1-pyrenyl)ethyl] ether (B1PEE).[21]

Experimental Section

B1PEE was synthesized in analogy with the method described by Becker.[15] *meso*- and *rac*-B1PEE obtained upon chromatography on silica with 80/20 toluene–hexane eluent were assigned by using ^{1}H NMR and ^{13}C NMR spectroscopy. Compared to *rac*-B1PEE, the meso diastereoisomer shows an upfield absorption of the methine carbons in the ^{13}C NMR spectrum and a downfield absorption of the methine hydrogens in the ^{1}H NMR spectrum. All systems of type I show this effect. *meso*- and *rac*-D1PP were synthesized according to the method described by Ito.[8] The diastereoisomers were separated by chromatography on alumina with 97/3 hexane–tetrahydrofuran eluent. *meso*- and *rac*-D1PP were assigned on the basis of the methylene and methine absorption signals in the ^{1}H NMR spectrum.

The ^{1}H NMR spectra were taken on a Bruker WM 250 (250 MHz) All fluorescence spectra were taken on a Spex Fluorolog. The apparatus used for the single-photon-counting measurements is described elsewhere.[22] All fluorescence measurements were performed in isooctane.

Table I
^{1}H NMR Data of *rac*- and *meso*-D1PP at Room Temperature in $CDCl_3$

δ	multiplicity	origin	J, Hz
		rac-D1PP	
1.49	d	CH_3	^3J = 6.90
2.53	$AA'XX'$	CH_2	$J_{AX} = J'_{AX}$ = 7.40
3.71	$AA'XX'$	CH	
7.05–8.22	m	arom H	
		meso-D1PP	
1.54	d	CH_3	^3J = 6.86
2.44	ABX_2	CH_2	J_{AX} = 7.38
3.95	ABX_2	CH	J_{BX} = 7.39
7.93–8.22	m	arom H	

Results and Discussion

Identification of *meso*- and *rac*-D1PP can be achieved by looking at the ^{1}H NMR absorption signals of the methine and methylene protons. In the case of *meso*-D1PP these four protons form an ABX_2 type spectrum while in the case of *rac*-D1PP an $AA'XX'$ type spectrum is observed. These spectra are presented in Figures 1 and 2. In analogy with the method developed by Bovey[14] the vicinal spin–spin coupling constants between the methine and the methylene protons are used in the conformational analysis. Considering the rapid conformational motion on the NMR time scale, the observed coupling constant[3] J_{obsd} is the average coupling constant which originates from the nine possible chain conformations.

$$^3J_{obsd} = \sum_{i=1}^{9} X_i {}^3J_i$$

X_i and ^3J_i represent the mole fraction and the vicinal coupling constant of conformation i. A value of 10 Hz is taken for $^3J_{trans}$–$^3J_{gauche}$. It is assumed that the values of the trans and gauche coupling constants $^3J_{trans}$ and $^3J_{gauche}$ are the same for all conformations. With these assumptions, the conformational distribution can be calculated. The results are in agreement with those of conformational analysis of similar compounds.[5,14,16,19,20]

On the basis of the $^3J_{obsd}$ coupling constants, it is concluded that at room temperature the TT and GG conformations are the most stable conformations of *rac*-D1PP (Figure 3). The ^{1}H NMR data of *rac*-D1PP are given in Tables I and II. The pyrene chromophores in the TT conformation of *rac*-D1PP show a small overlap as can easily be seen on molecular models. This results in the spreading of the absorption signals of the aromatic protons from 7.0 to 8.2 ppm at room temperature in deuterated chloroform. It is therefore possible to attribute all the protons in the aromatic region (Figure 1). Conformational

0024-9297/85/2218-1026$01.50/0 © 1985 American Chemical Society

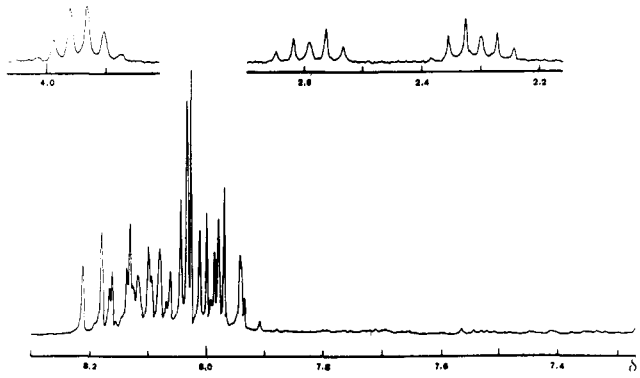

Figure 1. ^{1}H NMR spectrum of the methine, methylene, and aromatic protons of *meso*-D1PP in $CDCl_3$ at room temperature.

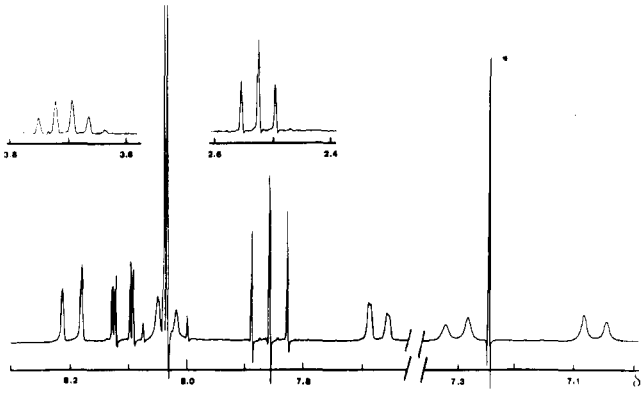

Figure 2. ^{1}H NMR spectrum of the methine, methylene, and aromatic protons of *rac*-D1PP in $CDCl_3$ at room temperature.

Table II
^{1}H NMR Data of the Aromatic Protons of *rac*-D1PP at Room Temperature in $CDCl_3$

δ	multiplicity	origin	J, Hz
8.19, 8.03	d, d	H_2, H_3	$J_{H_2-H_3}$ = 8.2
8.02, 8.05	AB	H_4, H_5	J_{AB} = 9.0
8.11	d *x*d	H_6	$J_{H_6-H_7}$ = 7.6
			$J_{H_6-H_8}$ = 1.2
7.86	t	H_7	$J_{H_7-H_6}$ = 7.6
7.67	d *x*d	H_8	$J_{H_8-H_7}$ = 7.6
			$J_{H_8-H_6}$ = 1.2
7.30, 7.07	d, d	H_9, H_{10}	$J_{H_9-H_{10}}$ = 9.4

distribution of *rac*-D1PP has also been studied as a function of temperature. Calculation of the conformational distribution according to the method described above could only be done at a few temperatures because of peak broadening. However, the enlargement of the absorption domain of the aromatic protons varies strongly with temperature. The absorption of the proton in position 10 as a function of temperature can be used as a sensitive measure to determine the percentage of TT conformation present. With this method, the conformational distribution has been determined in a small temperature range in deuterated cyclohexane. With the van't Hoff relation $\Delta H°$ and $\Delta S°$ were determined for this equilibrium. The respective values are 5.8 kJ mol^{-1} and 8.4 J mol^{-1} K^{-1}. On the basis of these data the conformational distribution shifts at lower temperature completely in favor of the TT conformation. At 183 K the conformational distribution was found to be 94% TT and 6% of the GG conformation. These results must be interpreted with caution because they do not take into account the possible orientations of the pyrene chromophore.

In the case of *meso*-D1PP the conformational distribution is shifted entirely in favor of the TG conformation. The TT conformation is only present in a small proportion

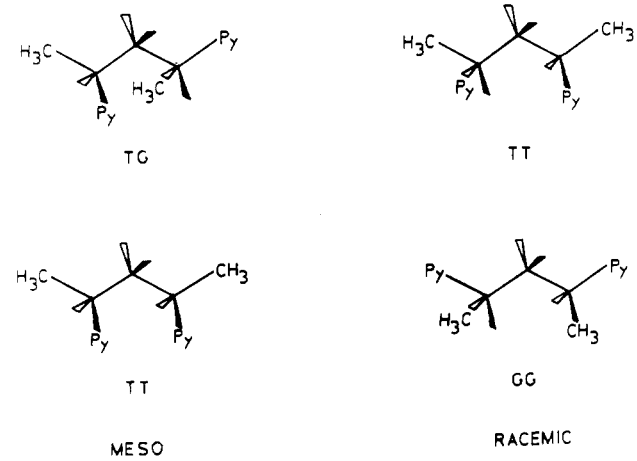

Figure 3. The four most stable chain conformations of the meso (TG and TT) and racemic diasteroisomers (TT and GG).

Table III
^{1}H NMR Data of the Aromatic Protons of *meso*-D1PP at Room Temperature in $CDCl_3$

δ	multiplicity	origin	J, Hz
8.19, 8.03	d, d	H_2, H_3	$J_{H_2-H_3}$ = 8.1
8.02, 8.05	AB	H_4, H_5	J_{AB} = 9.0
8.15	d *x*d	H_6	$J_{H_6-H_7}$ = 7.6
			$J_{H_6-H_8}$ = 1.4
7.97	t	H_7	$J_{H_7-H_6}$ = 7.6
8.12	d *x*d	H_8	$J_{H_8-H_7}$ = 7.6
			$J_{H_8-H_6}$ = 1.9
8.10, 7.96	d, d	H_9, H_{10}	$J_{H_9-H_{10}}$ = 9.4

Table IV
Conformational Distribution of *meso*- and *rac*-D1PP in Different Solvents and Compared to the Hildebrand Solvent Parameter δ[a]

D1PP	solv	% conformn	temp, K	δ(H)
racemic	octane-d_{18}	14 (GG)	323	7.1
racemic	cyclohexane-d_{12}	24 (GG)	323	8.0
racemic	chloroform-d_1	50 (GG)	323	9.1
racemic	THF-d_8	50 (GG)	323	9.1
meso	chloroform-d_1	99 (TG)	298	9.3
meso	cyclohexane-d_{12}	94 (TG)	298	8.2

[a] Reference 23. Identical δ values are assumed for deuterated and nondeuterated solvents.

at room temperature. The ^{1}H NMR data of meso-D1PP are summarized in Tables I and III. The absorption signals of the aromatic protons are all situated between 7.9 and 8.2 ppm, reflecting the very small percentage of TT conformation where there should be already in the ground state a large overlap between the pyrene chromophores (Figure 1).

The conformational distribution of *meso*- and *rac*-D1PP has also been determined in several solvents. The data in Table IV show an important change in the contribution of the GG conformation of *rac*-D1PP. The solvation of the pyrene chromophore is much better in solvents such as chloroform and tetrahydrofuran (THF) compared to alkane solvents. The contribution of the GG conformation will be larger in these solvents because in this conformation contact with the solvent molecules and the pyrene chromophore is better than in the TT conformation. In the case of *meso*-D1PP a similar but smaller effect is observed. The TG conformation becomes even more predominant in chloroform because of the same reason as mentioned above. In both solvents, however, the TG conformation remains the most important one. The conformational distribution in different solvents can be correlated to the Hildebrand solvent parameter (Table IV).[23]

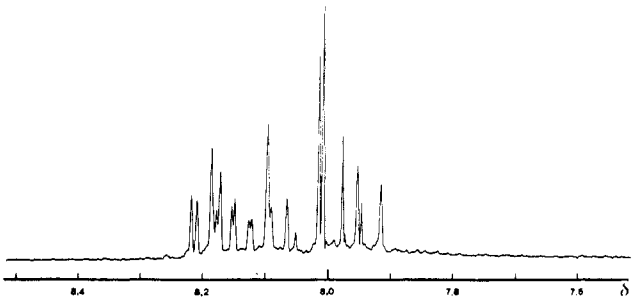

Figure 4. ^{1}H NMR spectrum of the aromatic protons of *meso*-B1PEE in $CDCl_3$ at room temperature.

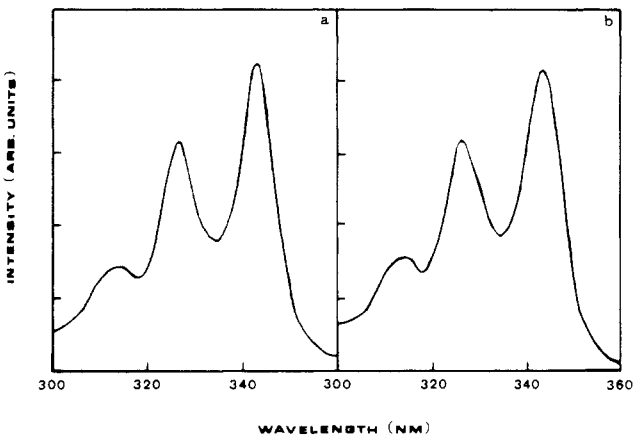

Figure 5. Fluorescence excitation spectra of *meso*-B1PEE as a function of the analysis wavelength (a: 450 nm; b: 530 nm) at room temperature.

The presence of an oxygen atom in *meso*- and *rac*-B1PEE makes it impossible to determine the conformational distribution using the same method as with D1PP. However, through a comparative ^{1}H NMR study it is possible to obtain some information. The ^{1}H NMR and ^{13}C NMR data of both *meso*- and *rac*-B1PEE have been published elsewhere.[21] In the case of *meso*-B1PEE it is most likely that the TG conformation is predominant. If a large amount of the TT conformation were present, the ^{1}H NMR spectrum should show strong shifts in the aromatic region compared to *meso*-D1PP (Figure 4). Also an important electronic interaction should result if the TT conformation were present in a large amount. The fluorescence excitation spectra at 298 K as a function of the analysis wavelength show no such effect, indicating no measurable contribution of the TT conformation in the ground state at that temperature (Figure 5). At low temperature (180 K) the ^{1}H NMR spectrum of *meso*-B1PEE in THF shows a strong broadening of the aromatic absorption signals indicating the existence of different rotamers of the TG conformation (Figure 6). In the case of *rac*-B1PEE the aromatic ^{1}H NMR signals are spread out as was observed for *rac*-D1PP but to a much lesser extent. The quantitative interpretation of this is difficult because of the difference in bond length between ether bonds and carbon–carbon bonds. In general, carbon–oxygen bonds in ethers are shorter (1.43 Å) than paraffinic carbon–carbon bonds (1.54 Å).[23] This causes the pyrene chromophores to be closer together in the TT conformation of *rac*-B1PEE, producing a stronger steric effect and forcing other TT rotamers to become more populated (Figure 7). In these other rotamers, the pyrene chromophores are rotated away from each other. This is indicated by low-temperature ^{1}H NMR. At 180 K three separate signals were observed for the methine hydrogen and methyl hydrogen absorption signals in THF d_8 and CD_2Cl_2.

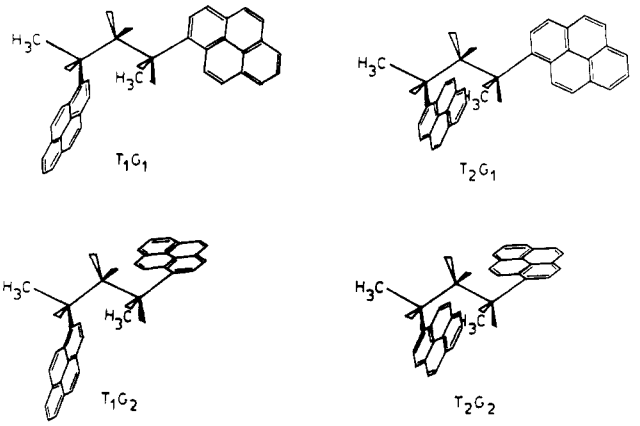

Figure 6. The four possible rotamers of the chain conformation TG of the meso diasteroisomer.

Table V
Emission Maxima and Fwhh of the Excimer Band of *meso*-D1PP and *meso*-B1PEE as a Function of Temperature

	meso-D1PP	*meso*-B1PEE
λ_{max}(298 K), nm	480	472
λ_{max}(183 K), nm	500	492
fwhh(298 K), cm^{-1}	4300	4800
fwhh(183 K), cm^{-1}	3800	4400

Table VI
Variation of the Decay Parameters as a Function of the Analysis Wavelength (aw) in the Excimer Region of *meso*-B1PEE at Room Temperature[a]

aw, nm	α_1	τ_1	α_2	τ_2	Q_2/Q_1
430	0.26	46.3	0.16	78.3	1.04
450	0.19	46.8	0.16	79.8	1.44
470	0.14	45.7	0.21	82.4	2.70
490	0.09	46.8	0.41	81.0	7.90
510	0.09	46.8	0.43	83.7	8.57

[a] $Q_i = \alpha_i\tau_i/\sum_{i=1}^{2}\alpha_i\tau_i$. The fluorescence decay $i(t)$ was analyzed as $i(t) = \sum_{i=1}^{2}\alpha_i \exp(-t/\tau_i)$.

Table VII
Variation of the Decay Parameters as a Function of the Analysis Wavelength (aw) in the Excimer Region of *meso*-D1PP at Room Temperature[a]

aw, nm	α_2	τ_2	α_3	τ_3	Q_3/Q_2
450	0.30	79.6	0.45	160.8	1.50
470	0.21	80.4	0.54	161.1	5.16
490	0.20	79.9	0.56	157.9	5.56
510	0.18	79.9	0.57	159.8	6.70
530	0.09	80.4	0.64	151.5	15.16

[a] $Q_i = \alpha_i\tau_i/\sum_{i=1}^{3}\alpha_i\tau_i$. The fluorescence decay $i(t)$ was analyzed as $i(t) = \sum_{i=1}^{3}\alpha_i \exp(-t/\tau_i)$.

With ^{13}C NMR the conformational distribution was found to be 64%, 18%, and 18% for the three conformations at 173 K in THF-d_8. This clearly indicates the importance of rotamers at that temperature.

The fluorescence spectra of *meso*-D1PP and *meso*-B1PEE as a function of temperature show very similar behavior. In both cases the fluorescence spectra at room temperature show only excimer emission (Figures 8 and 9). The excimer band itself is very broad and shows a strong bathochromic shift as a function of temperature (Table V). The broad excimer band suggests the existence of more than one excimer. With the time-correlated single-photon-counting technique, fluorescence decay measurements were performed on both compounds. Analyzing the fluorescence decay at different wavelengths in the excimer band indicated the existence of two decaying

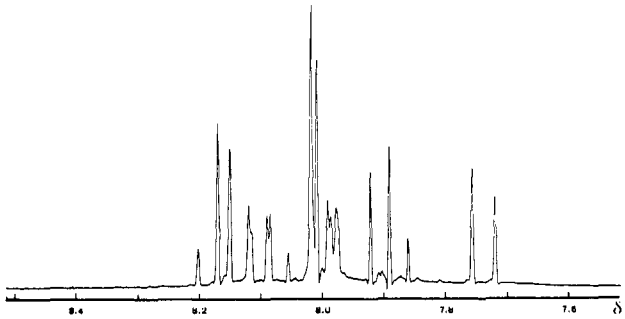

Figure 7. ^1H NMR spectrum of the aromatic protons of *rac*-B1PEE in $CDCl_3$ at room temperature.

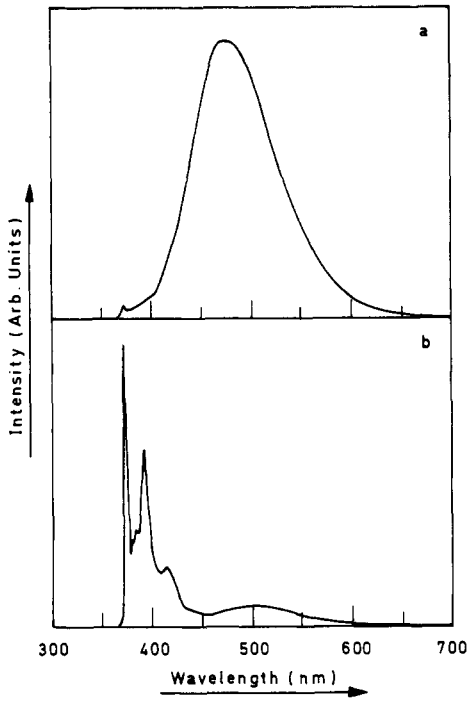

Figure 8. Fluorescence spectra of *meso*-D1PP at different temperatures: (a) 298 and (b) 183 K.

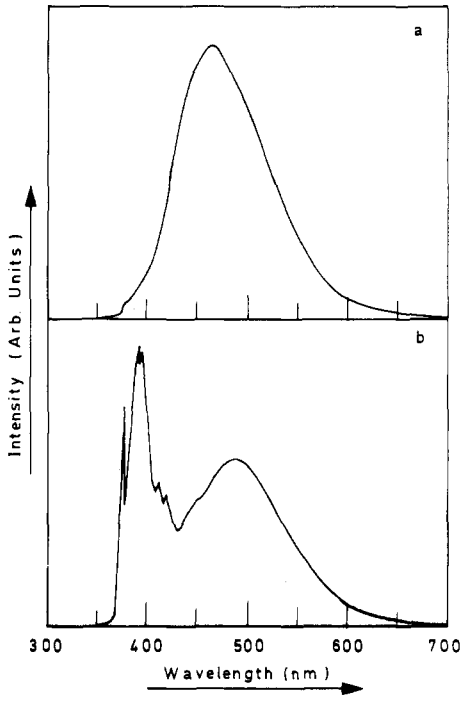

Figure 9. Fluorescence spectra of *meso*-B1PEE at different temperatures: (a) 298 and (b) 183 K.

Table VIII
Possible Rotamers of the TG Conformation and Their Corresponding Excimer Conformation[a]

ground-state conformn	excimer conformn
T_1G_1	T_1T_1 (eclipsed)
T_2G_1	T_2T_1 (staggered)
T_1G_2	T_1T_2 (staggered)
T_2G_2	T_2T_2 (eclipsed)

[a] Subscript 1: pyrene *peri*-hydrogen is oriented toward the methine hydrogen. Subscript 2: pyrene *peri*-hydrogen is oriented between methyl and methylene group of the chain.

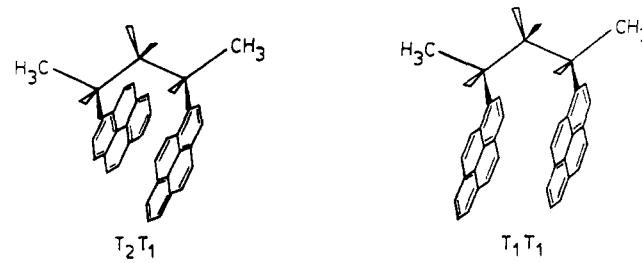

Figure 10. Possible structure for the eclipsed (T_1T_1) and staggered (T_2T_1 or T_1T_2) excimer conformation.

species with a different decay time and a different spectral distribution. This suggests that the two excimers have a different geometry (Tables VI and VII). Analysis of the fluorescence decay of *meso*-D1PP and *meso*-B1PEE in the monomer region (378 nm) shows two excimer-forming components in the whole temperature region studied (183–233 K for *meso*-B1PEE and 203–263 K for *meso*-D1PP). At higher temperatures the analysis at 378 nm becomes impossible because of the low fluorescence intensity and overlap from the excimer band. The NMR study shows that in the studied temperature range only one chain conformation is to be considered. Steric hindrance caused by the pyrene *peri*-hydrogen with the backbone chain causes the rotation of the pyrene group to occur more slowly than the rotation in the chain (from TG to the TT excimer conformation). This can easily be seen by using space-filling molecular models. The two decay components in the monomer region can then be interpreted as different rotamers of the TG conformation. Because of the slow pyrene rotation, different rotamers will form geometrically different excimers. In the TG conformation four different rotamers are possible (Figure 6). Two of these can form an eclipsed excimer while the remaining two form a staggered excimer. Table VIII shows the four possible rotamers and their corresponding excimer conformations. Note that the eclipsed excimer conformations T_1T_1 and T_2T_2 are in fact different conformations due to the position of the methylene group. The steric interaction between the methylene group and the *peri*-hydrogens makes the T_2T_2 a highly unstable conformation compared to the T_1T_1 conformation. The two staggered excimer conformations are identical (Figure 10). The two orientations (subscript 2) of the pyrene chromophores produce a steric crowding effect making the T_2G_2 conformation less probable. One of the observed excimers is then formed by the T_1G_1 conformation and the other is formed by either the T_2G_1 or the T_1G_2 conformation or both. However, to form an appreciable overlap of the two chromophores (more than one ring of the chromophore) the T_2G_1 has to undergo a rotation of less than 120° toward the TT conformation. To produce the same overlap from the T_1G_2 rotamer, a rotation of more than 120° (past the TT conformation) is necessary. Although both rotamers (T_2G_1 and T_1G_2) form the same excimer, they may act as kinetically different species. In the case of *meso*-B1PEE

Table IX
Activation Energies (E_a), Preexponentials (A), and Rate Constants of Excimer Formation (k_{DM}) of *meso*-D1PP and *meso*-B1PEE

	meso-D1PP	*meso*-B1PEE
E_{a_1}, kJ mol^{-1}	11.7	8.3
A_1	1.6×10^{10}	6.5×10^{10}
E_{a_2}, kJ mol^{-1}	20.8	18.7
A_2	1.5×10^{12}	3.3×10^{12}
k_{DM_1}(298 K), s^{-1}	2.9×10^{8}	1.5×10^{9}
k_{DM_2}(298 K), s^{-1}	4.8×10^{8}	1.8×10^{9}

there is some indication that the pyrene group in the G position is lying in the same plane as the ether chain.[20] If this is so, the number of conformational possibilities is diminished to two. Only the T_1G_1 and the T_2G_1 conformation should be present. The kinetic data in Table IX could then be adequately explained with these two conformations. The lower activation energy is caused by the partial rotation necessary to form the staggered excimer from the T_2G_1 rotamer. The higher activation energy could be explained by the rotation to form the eclipsed excimer from the T_1G_1 rotamer. However, if the T_1G_2 rotamer is also present, the high activation energy could be related to the kinetically similar T_1G_1 and T_1G_2 rotamers. Since, in the case of *meso*-D1PP no obvious reason can be found why either the T_1G_2 or the T_2G_1 rotamer is more stable, the second explanation is presently favored.

Conclusion

The compounds investigated here are a model for the isotactic and heterotactic diads of poly(1-vinylpyrene). The already complex kinetic behavior of these fairly simple molecules suggests a highly complex kinetic behavior of the corresponding atactic polymer. The spectral and kinetic differences between *meso*-B1PEE and *meso*-D1PP indicate that B1PEE should not be considered as an appropriate model for poly(1-vinylpyrene).

A conformational study of bichromophoric compounds is a necessity whenever intramolecular excimer formation is investigated. Conformational data are useful to explain the sometimes complex excited-state behavior of these compounds. If the chromophores investigated are not symmetrically substituted, the existence of several rotamers should be taken into account. This also includes the possibility of having more than one excimer species.

Acknowledgment. P.C. thanks I.W.O.N.L. for a doctoral fellowship. We thank the F.K.F.O. and the University Research Fund for Financial support of the laboratory. Q.F.Z. thanks the Academia Sinica and the N. F.W.O. for financial support during his stay in Leuven. N.B. is a research associate of the National Fund for Scientific Research.

References and Notes

(1) Ghiggino, K. P.; Roberts, A. J.; Phillips, D. *Adv. Polym. Sci.* **1981**, *40*, 69.
(2) Klöppfer, W. *Ann. N.Y. Acad. Sci.* **1981**, *366*, 373.
(3) MacCallum, J. R. *Eur. Polym. J.* **1981**, *17*, 209.
(4) De Schryver, F. C.; Put, J. *Ind. Chim. Belge.* **1972**, *37*, 1107.
(5) De Schryver, F. C.; Vandendriessche, J.; Toppet, S.; Demeyer, K.; Boens, N. *Macromolecules* **1982**, *15*, 406.
(6) Monnerie, L.; Bokobza, L.; De Schryver, F. C.; Moens, L.; Van der Auweraer, M.; Boens, N. *Macromolecules* **1982**, *15*, 64.
(7) De Schryver, F. C.; Demeyer, K.; Van der Auweraer, M.; Quanten, E. *Ann. N.Y. Acad. Sci.* **1981**, *366*, 93.
(8) Ito, S.; Yamamoto, M.; Nishijima, Y. *Bull. Chem. Soc. Jpn.* **1981**, *54*, 35.
(9) De Schryver, F. C.; Demeyer, K.; Toppet, S. *Macromolecules* *1983*, *16*, 89.
(10) Vandendriessche, J.; Palmans, P.; Toppet, S.; Boens, N.; De Schryver, F. C. *J. Am. Chem. Soc.*, in press.
(11) Evers, F.; Kobs, K.; Memming, R.; Terrel, D. R. *J. Am. Chem. Soc.* **1983**, *105*, 5988.
(12) De Schryver, F. C.; Demeyer, K.; Vandendriessche, J.; Collart, P.; Boens, N. *J. Polym. Photochem.* **1985**, *6*, 215.
(13) Longworth, J. W.; Bovey, F. A. *Biopolymers* **1966**, *4*, 1115.
(14) Bovey, F. A.; Hood, F. P., III; Anderson, E. W.; Snyder, L. C. *J. Chem. Phys.* **1965**, *42*, 3900.
(15) Becker, H. D.; Anderson, K. *J. Org. Chem.* **1982**, *47*, 354.
(16) Moritani, T.; Fujiwara, Y. *J. Chem. Phys.* **1973**, *59*, 1175.
(17) Jasse, B.; Lety, A.; Monnerie, L. *J. Mol. Struct.* **1973**, *18*, 413.
(18) Yoon, D. Y.; Sundararayan, P. R.; Flory, P. J. *Macromolecules* **1975**, *8*, 776.
(19) Ito, S.; Yamamoto, M.; Nishijima, Y. *Bull. Chem. Soc. Jpn.* **1982**, *55*, 363.
(20) Pajot, E. Thèse Dr. Ir. Université de Paris 6, 1983.
(21) Collart, P.; Demeyer, K.; Toppet, S.; De Schryver, F. C. *Macromolecules* **1983**, *16*, 1390.
(22) Desie, G.; Boens, N.; Van den Zegel, M.; De Schryver, F. C. *Anal. Chim. Acta*, in press.
(23) "Handbook of Chemistry and Physics"; CRC Press: Boca Raton, FL, 1979-1980; p C372.

Inverse Gas Chromatography. 2. The Role of "Inert" Support†

Timothy W. Card, Zeki Y. Al-Saigh, and Petr Munk*

Department of Chemistry and Center for Polymer Research, University of Texas, Austin, Texas 78712. *Received July 30, 1984*

ABSTRACT: Retention volumes of nonpolar *n*-hexane, moderately polar ethyl acetate, and strongly polar ethanol were measured on chromatographic columns of Chromosorb W-Aw-DMCS treated, uncoated by any polymer, and on columns coated with polyisobutylene and poly(methyl acrylate), respectively. For each column and probe, the dependence on the amount injected was studied. The DMCS treatment seemed to produce some poly(dimethylsiloxane) attached to the uncoated support; this led to (linear) retention of all probes. In addition, the remaining strongly polar groups on the surface of the support interacted with polar probes extensively and in a strongly nonlinear way. To obtain meaningful data for the retention of the probes, the retention volumes measured on the uncoated column had to be subtracted from the data for coated columns. For polyisobutylene, the new procedure yielded specific retention volumes V_g that were independent of the injected amount, flow rate, and polymer loading of the column for all probes.

Introduction

In recent years, inverse gas chromatography (IGC) has become an almost routine method for obtaining thermodynamic data on polymeric systems.[1-31] The method is termed "inverse" because, unlike standard gas chromatography, it is the stationary phase (polymer or polymer blend) which is of interest. Despite broad usage, the method remains complicated by experimental and theoretical factors that are not completely understood. Some

† *Macromolecules* 1984, *17*, 803 is considered to be part 1 of this series.

0024-9297/85/2218-1030$01.50/0 © 1985 American Chemical Society